

Effects of interadsorbate interactions on surface resistivity: Oxygen on sulfur-predosed Cu(100)

Chang Liu and R. G. Tobin^{a)}*Department of Physics and Astronomy, Tufts University, Medford, Massachusetts 02155, USA*

(Received 31 March 2008; accepted 14 May 2008; published online 23 June 2008)

Measurements of surface resistivity as a function of coverage for oxygen adsorbed on sulfur-predosed Cu(100) films reveal two types of interactions between sulfur and oxygen: S–O repulsion and short-range suppression of the surface resistivity change induced by oxygen adsorption. The repulsive interaction causes oxygen atoms to first occupy adsorption sites far from the sulfur atoms, beyond second-nearest-neighbor sites, where the oxygen-induced surface resistivity is unaffected by sulfur. As a result the low-coverage variation of surface resistivity with oxygen coverage is indistinguishable from the linear dependence observed for oxygen on clean Cu(100). As the oxygen coverage increases, oxygen begins to occupy sites close to sulfur. At the nearest-neighbor sites, the resistivity change due to added oxygen is completely suppressed, and the sample resistance levels off, remaining unchanged even as oxygen continues to adsorb. This resistivity suppression may involve both a reduction of oxygen's direct effect on the resistivity and an oxygen-induced reduction in the resistivity due to the already adsorbed sulfur. With increasing sulfur precoverage both the maximum resistivity change and the oxygen coverage at which the leveling occurs decrease, because the number of sites unaffected by sulfur is reduced. Both the sulfur-oxygen repulsion and the resistivity suppression presumably arise from a through-metal coupling involving adsorbate-induced modifications of the local electronic structure. © 2008 American Institute of Physics. [DOI: 10.1063/1.2940336]

INTRODUCTION

Interactions between adsorbed molecules on metal surfaces have been investigated through measurements of surface resistivity, which can also provide information pertinent to such fields as tribology, thin film growth, sensing, and nanotechnology. Surface resistivity can provide insight into adsorption kinetics,^{1–3} electromigration,⁴ atomic-scale friction,^{5–8} and adsorbate effects on the electrical resistance of metallic nanowires^{9–11} and carbon nanotubes.^{12,13}

Current understanding of surface resistivity is based on the model of electron-adsorbate scattering, first proposed by Fuchs¹⁴ and Sondheimer,¹⁵ and elaborated by Persson and Volokitin.^{6,16–20} Chemisorbed molecules, acting as scattering centers, diffusely scatter conduction electrons in the metal from the local potential of the adsorbates, adding to the surface resistivity. The change in dc resistivity of a metallic film has the form²¹

$$\frac{\Delta\rho}{\rho_B} = \frac{3}{16} \frac{\ell_B}{t} n_a \Sigma, \quad (1)$$

where ρ_B is the bulk resistivity, t is the thickness of the metal film, n_a is the surface density of the adsorbates, ℓ_B is the bulk electron mean free path, and Σ is the scattering cross section per adsorbate. Because the resistivity change $\Delta\rho$ arises from the direct interaction of the conduction electrons with the adsorbate, it is a first layer effect. Subsequent layers grown

on top of the first chemisorbed layer have negligible effect on the metal's conductivity.³

For a single adsorbed species with no interadsorbate interactions the cross section Σ is constant and the surface resistivity increases linearly with the coverage, as observed for CO on Cu,^{2,22,23} C₂H₂ on Cu(100),² and O on Cu(100).²⁴ More complex dependences can result from multiple species, as we have observed for CO on stepped Cu(100),²³ or from strong interactions that modify the cross section, as seen for CO with coadsorbed C₂H₄ on Cu(111),²⁵ where the C₂H₄ increases the surface resistivity caused by CO, or for S on Cu(100),²⁴ where interactions within the adlayer reduce the scattering cross section and cause the resistivity to level off at high coverage.

We report experiments on the changes in surface resistivity that result from adding adsorbed oxygen to a Cu(100) surface predosed with sulfur. The results show a nearly complete suppression of the surface resistivity increase due to the oxygen, but only when oxygen atoms adsorb on sites immediately adjacent to sulfur atoms (first-nearest-neighbor sites). For oxygen on second-nearest-neighbor sites the resistivity change is reduced by about 30%, relative to oxygen on clean Cu(100), and for larger S–O distances there is no detectable suppression. Because of a repulsive interaction between oxygen and sulfur, the effects of the resistivity suppression appear only at the highest oxygen coverages.

EXPERIMENTS

Details of the sample preparation procedures have been reported elsewhere.^{24,26,27} The copper films were grown *in*

^{a)}Author to whom correspondence should be addressed. Electronic mail roger.tobin@tufts.edu.

situ in ultrahigh vacuum (UHV) on $9 \times 28 \text{ mm}^2$ Si(100) substrates. Contact strips (50 nm Ag on top of 10 nm Cr) were deposited *ex situ*, and each substrate was etched for 60 s in a 10% aqueous solution of HF to remove the native oxide and passivate the surface by terminating the dangling Si bonds with H atoms.²⁸ After etching, the sample was loaded within a few minutes into a high-vacuum load lock for transport into the UHV chamber. For Si(111) a more perfect H-terminated surface can be obtained by the use of NH_4F buffered HF,^{29,30} but for Si(100) anisotropic etching can lead to roughening via the formation of (111) microfacets.^{31–33} In any case the H-terminated Si(100) surface prepared by etching in dilute HF has been shown to be an excellent substrate for growing epitaxial Cu(100) films.^{26,34,35}

After transfer into UHV the substrate was heated to 450 K to desorb the hydrogen, and maintained at that temperature for 15 min to allow the hydrogen partial pressure in the chamber, as measured with a residual gas analyzer, to return to its baseline level. Copper was then deposited by resistive thermal evaporation from a well-outgassed filament at a rate of 0.01–0.1 nm/s with the substrate temperature regulated at $298 \pm 2 \text{ K}$. During deposition the chamber pressure was on the order of 10^{-9} Torr. Previous x-ray diffraction studies of films grown under conditions nominally identical to those used for current experiments²⁶ showed fully epitaxial growth, the Cu[100] direction aligned with Si[100]. Atomic force microscopy showed a root-mean-square surface roughness of 1–2 nm. X-ray diffraction measurements on more recently grown samples have shown less perfect crystallinity, but still indicate that the films are highly textured with the [100] direction normal to the surface within $\pm 7^\circ$.

The films' resistance was measured with an ac four-terminal technique, using a 1.0 mA rms current modulated at 3 kHz. Electrical contact was made via copper clips pressing on the contacts, with separate electrical connections for the current and voltage leads. The resistance of the film was continuously monitored during the deposition, and was 3–4 Ω at $T=298 \text{ K}$ immediately after deposition. This resistance is several times higher than would be expected for pure bulk Cu of the nominal sample dimensions, probably due in part to a high resistance buffer layer at the Si–Cu interface,²⁶ and in part to the relatively high density of defects on the sample surface,^{23,26} as well as to possible impurities and defects in the bulk.

After Cu deposition, the sample was cooled to 273 K, to be consistent with the previous experimental conditions for O/Cu(100) and S/Cu(100),²⁴ and its temperature regulated within $\pm 2 \text{ K}$. Sulfur adsorption was achieved by admitting H_2S gas through a multihole effusive doser with an enhancement factor of 15–20.³⁶ H_2S is known to dissociate on Cu(100) and hydrogen desorbs, leaving adsorbed S on the surface.^{37,38} The S coverage was determined from the S(152)/Cu(60) Auger ratio, using the calibration given in Ref. 38. Each Si/Cu sample was used for only one adsorption sequence; for each experimental run a new Si substrate was prepared and a new Cu film deposited. Five runs were carried out with no sulfur dosing to verify experimental re-

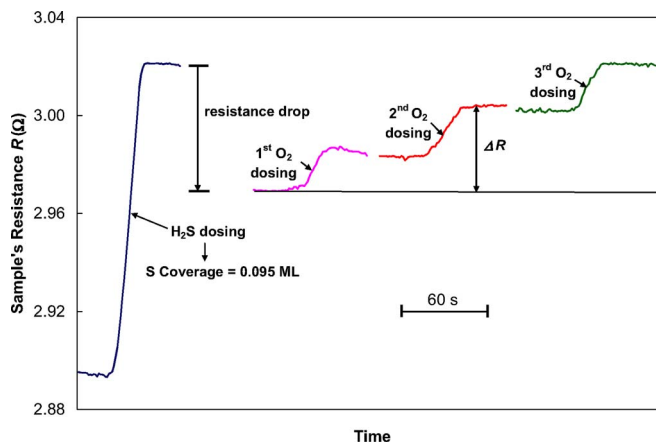


FIG. 1. (Color online) Resistance vs time for a typical adsorption sequence for 0.095 ML sulfur precoverage, showing the initial sulfur dose and three subsequent oxygen doses. An Auger spectrum was measured after each dose. The interval between doses was approximately 30 min.

producibility, and one run at each of three different sulfur coverages, on separate but identically prepared Cu(100) films.

After the film was prepared, and if necessary dosed with sulfur, the sample was dosed with oxygen several times until no further increase in oxygen coverage was observed, also through the same multihole effusive doser with the resistance monitored continuously. Residual gas analysis during oxygen dosing showed no detectable SO or SO_2 , and Auger spectroscopy showed no increase in the S level on the sample following oxygen dosing, so we see no evidence of contamination resulting from the use of the same doser for both sulfur and oxygen exposures. Oxygen coverages were determined from the O(512)/Cu(920) Auger ratio, using the calibration from Refs. 39 and 40. To improve accuracy, especially at low oxygen coverage, the oxygen peak-to-peak signal was determined from a fit to a Gaussian line shape.

Figure 1 shows a sequence of resistance vs. time traces for a typical experimental run, including both the initial sulfur dose and a series of sequential oxygen doses. An Auger spectrum was measured after each dose, and the time between the completion of one trace and the start of the next was typically about 30 min. The oxygen-induced resistance change was found by comparing the resistance after the oxygen dose to that before the first oxygen exposure. A decrease in resistance between the end of the sulfur dose and the beginning of the first oxygen dose, clearly visible in Fig. 1, was consistently observed and is not understood. There was no indication that sulfur was lost from the surface during the experiment; the resistance drop may result from reorganization in the sulfur layer.

RESULTS AND ANALYSIS

Figure 2 presents the oxygen-induced resistance change of the sulfided Cu film as a function of oxygen coverage for experiments on both clean and sulfur-predosed Cu(100). For oxygen on clean Cu(100), the resistance exhibits the linear behavior observed in previous experiments,²⁴ indicating that the adsorbed oxygen atoms act as independent noninteracting scattering centers for the metal's conduction electrons, with a

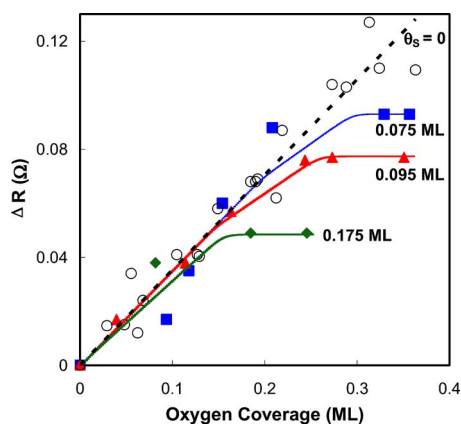


FIG. 2. (Color online) Surface resistance change (ΔR) vs oxygen coverage on a 50 nm Cu(100) film with different sulfur precoverages (θ_s) at $T = 273$ K. The solid lines are the best-fit resistance-coverage curves obtained from the simulation described in the text. Compared to the linear coverage dependence without preadsorbed sulfur, interactions of S and O completely suppress the increase of surface resistance at high oxygen coverage until it levels off at a nearly constant maximum value.

constant scattering cross section Σ . On the sulfur-predosed samples, the same linear dependence is observed at low oxygen coverage, with the same slope. This behavior indicates that any influence of sulfur on oxygen's scattering, or of oxygen on sulfur's, is negligible at these coverages.

Above a threshold oxygen coverage, however, the resistance levels off at a nearly constant value, even as the oxygen coverage continues to increase. In this regime the interaction between sulfur and oxygen results in a near-zero resistivity change per additional oxygen atom. This dramatic suppression of oxygen's surface resistivity contribution may result from a combination of a sulfur-induced reduction in oxygen's electron-scattering cross section, and a reciprocal reduction of sulfur's cross section by oxygen. Both the threshold coverage and the corresponding maximum resistance change decrease as the sulfur precoverage is increased.

We attribute the plateau in the resistance-coverage curve to a short-range interaction between O and S that very strongly suppresses the effective resistance change when O adsorbs on sites immediately adjacent to sulfur atoms. Based on the threshold coverages in Fig. 2 and the sharpness of the transition between the low- and high-coverage regimes, we infer that virtually complete suppression acts on first-nearest-neighbor sites while there is a transitional region, corresponding to occupation of second-nearest-neighbor sites, where oxygen's resistivity change is partially suppressed. The sharpness of the transition indicates both the short range of the resistance-suppressing interaction and the existence of a S–O repulsion that causes oxygen to avoid sites near S atoms until all other sites have been occupied.

To quantify these conclusions we have carried out Monte Carlo simulations using phenomenological S–O interactions. Both sulfur⁴¹ and oxygen⁴⁰ occupy fourfold hollow sites on Cu(100). We represent the surface by a (24×24) square lattice with periodic boundary conditions; larger grids did not significantly change the results. We assume the following:

- (1) Sulfur atoms adsorb randomly, but with a minimum S–S separation of two lattice spacings, consistent with

TABLE I. Fitting parameters for the resistance contributions of the first- (C_1) and second-nearest-neighbor (C_2) sites, relative to the contribution of other sites without suppression. The three rows represent three different sulfur coverages.

S coverage (ML)	C_1	C_2
0.075 ± 0.003	0 ± 0.03	0.69 ± 0.07
0.095 ± 0.003	0 ± 0.02	0.66 ± 0.05
0.175 ± 0.009	0 ± 0.03	0.88 ± 0.06

a $p(2 \times 2)$ geometric structure for S on Cu(100).⁴¹ For each S coverage we carried out 100 runs to average over possible sulfur distributions.

- (2) Oxygen atoms sequentially occupy sites at the maximum available distance from the preadsorbed S atoms, with a minimum O–O distance of 1.4 lattice spacings, consistent with a $c(2 \times 2)$ ordered structure for O on Cu(100) at coverages lower than 0.34 ML.⁴⁰ To include the effects of multiple sulfur atoms we assumed a pairwise power law interaction potential between sulfur and oxygen, $U_{S-O} \propto r^{-n}$, so that the total potential at a particular site can be parameterized by an effective sulfur-oxygen distance,

$$r_{SO} = \left(\sum_{i=1}^{N_S} r_i^{-n} \right)^{-1/n}, \quad (2)$$

where r_i is the distance from the site to the i th S atom. Values of the exponent n smaller than four could not reproduce the sharp change in slope exhibited by the data in Fig. 2. All of the simulations shown were carried out with $n=6$, but no particular significance should be attached to this value, except that our data require a rather short-range interaction. While our model imposes a deterministic adsorption sequence, with sites farther from sulfur always occupied before closer ones, the only feature necessary to fit the data is that second- and first-nearest-neighbor sites to the sulfur are occupied in sequence and only after virtually all available more distant sites have been filled.

- (3) The resistance contribution for oxygen atoms two or more lattice spacings from S is the same as on clean Cu. For oxygen on second-nearest-neighbor sites the resistance change is a fraction C_2 and on first-nearest-neighbor sites a fraction C_1 of the clean-Cu value. For each sulfur coverage these two quantities are varied to give the best fit to the experimental resistance-coverage curve. They are the only adjustable parameters in the model.

The lines in Fig. 2 show the results of the best-fit simulations, and the best-fit values of the suppression parameters C_1 and C_2 for each sulfur coverage are given in Table I. The results are consistent with zero resistance change when oxygen is adsorbed on nearest-neighbor sites, while for second-nearest-neighbor sites the change is 10%–30% lower than for more distant sites. The best-fit values for the three sulfur coverages are consistent, except that for the highest sulfur coverage the simulation gives a best-fit value of C_2 of 0.9,

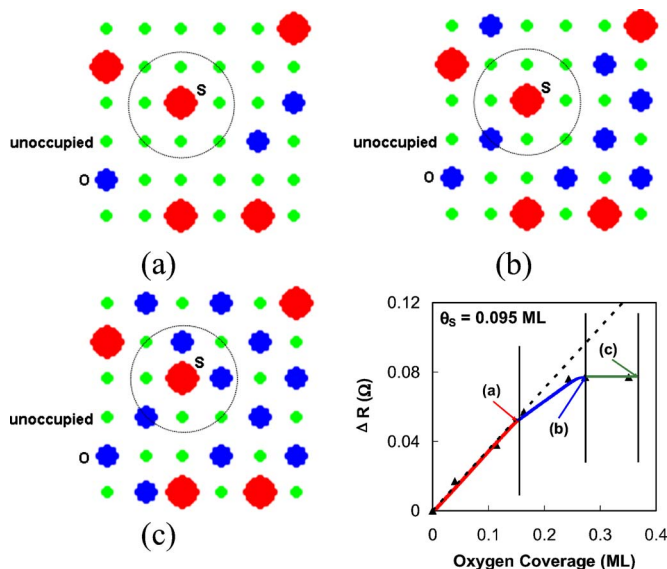


FIG. 3. (Color online) Sample simulated adsorbate distributions for three different oxygen coverages and the corresponding changes in surface resistance with oxygen coverage for 0.095 ML sulfur coverage (θ_S). Only a (6×6) section of the full (24×24) array is shown. (a) At low coverage, oxygen adsorbs far from the sulfur atoms, outside the effective range of suppression. The resistance change is not affected by sulfur. (b) With increasing oxygen coverage, O atoms occupy second-nearest-neighbor sites. The increase in resistance is slightly suppressed. (c) O atoms occupy first-nearest-neighbor sites. The resistance no longer increases with increasing oxygen coverage.

compared with 0.7 for the two lower sulfur coverages. This modest discrepancy may be an effect of sulfur-sulfur interactions, which become increasingly significant as the sulfur coverage increases.²⁴ But it could also be due to error in the determination of sulfur coverage. The data for the highest sulfur coverage can be reproduced with a value of $C_2=0.69$, consistent with the lower-coverage value, if the highest sulfur coverage is assumed to be 0.15 ML instead of 0.175 ML. We estimate the uncertainty in the coverage determination to be ± 0.009 ML, so an error of the necessary size is unlikely, but not excluded.

Figure 3 schematically depicts the evolution of the surface and the sample resistance with increasing oxygen coverage, for one representative simulation run at 0.095 ML sulfur coverage. [The curve in Fig. 3(d) is an average of 100 runs at the same coverage.] At low oxygen coverage [Fig. 3(a)], oxygen atoms adsorb only on sites outside the range of the resistance suppression, so the resistance is identical to what it would be on Cu(100) with no sulfur. Once the available unperturbed sites are filled, oxygen atoms begin to adsorb on second-nearest-neighbor sites [Fig. 3(b)] and the slope of the resistance-coverage curve decreases, because the resistance increase due to each newly adsorbed oxygen is $\sim 30\%$ smaller than at more distant sites. When no more second-nearest-neighbor sites are available, first-nearest-neighbor sites begin to fill [Fig. 3(c)], but because the resistance increase at these sites is completely suppressed by the oxygen-sulfur interaction, the resistance remains constant even as the oxygen coverage continues to increase.

This simple phenomenological model accurately reproduces both the shape of the resistance-coverage curve and

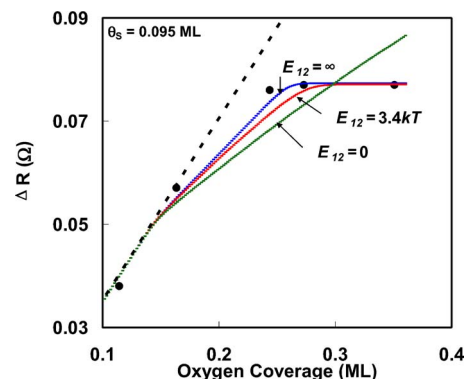


FIG. 4. (Color online) The simulated resistance change vs oxygen coverage for different values of the adsorption energy difference ΔE_{12} between first- and second-nearest-neighbor sites at 0.095 ML sulfur coverage (θ_S). For $\Delta E_{12} < 3.4kT$ significant deviations from the experimental data are observed.

the oxygen coverage at which the transition occurs. It is interesting that we can obtain this agreement only if oxygen atoms are allowed to occupy sites immediately adjacent to sulfur atoms, even though such small separations do not occur for either oxygen or sulfur adsorption alone. The S–O interaction, while clearly repulsive, is evidently not so repulsive as to prevent adsorption at such small separations. A sulfur anion (S^{2-}) on Cu(100) has an ionic radius of about 0.17 nm.⁴² For O/Cu(100), the O–Cu bond has a mixed ionic-covalent character,⁴³ and depending on the degree of ionicity the oxygen radius falls between 0.07 and 0.14 nm. The lattice spacing between nearest-neighbor sites is 0.25 nm. Possibly when the atoms are this close together, their bonds to the copper become less ionic, reducing their effective sizes, and making it possible for them to occupy sites at such small separation.

Our simulation shows the data are consistent with a rigid adsorption order—second- and first-nearest-neighbor sites are occupied in sequence, implying a difference in adsorption energy, ΔE_{12} , between the two sites. In effect, the deterministic simulations discussed above assume $\Delta E_{12}=\infty$, and the data are consistent with that extreme assumption. We can estimate a lower limit for ΔE_{12} by allowing mixing between first- and second-nearest-neighbor sites, determining their relative populations through a Boltzmann factor $e^{-\Delta E/kT}$, weighted by the relative number of available sites of each type. We carried out simulations with various values of $\Delta E_{12}/kT$, and find that the simulation deviates significantly from the data for ΔE_{12} smaller than about $3.4kT$, or 0.09 eV at our sample temperature of 273 K. Figure 4 presents the best-fit resistance versus coverage curves for $\Delta E_{12} = 0, 3.4kT$ and ∞ , respectively. In principle, a similar procedure could set a lower limit on the adsorption energy difference between second-nearest-neighbor and more distant sites, but because C_2 is only modestly smaller than one, we were not able to set any meaningful constraints on that quantity.

DISCUSSION

The experimental and simulated results clearly demonstrate the existence of two S–O interactions—resistivity sup-

pression and S–O repulsion. The suppression varies strongly with S–O distance: the oxygen-induced resistivity change is essentially zero on first-nearest-neighbor sites, while on second-nearest-neighbor sites it is reduced by only 10%–30%, compared to sites unaffected by sulfur. The sequential occupation of sites beyond second-nearest-neighbor, followed in sequence by second- and then first-nearest-neighbor sites, indicates a strong sulfur-oxygen repulsion. Both interactions must have their origins in a through-metal interaction between the adsorbed atoms, mediated by the electronic states of the metal.

A similar short-range repulsive interaction has also been observed for S and CO on Cu(100),⁴² but with some significant differences. For S and CO, Hu and Hirschmugl found that sulfur completely blocks the first-nearest-neighbor sites, and suppresses CO adsorption at second-nearest-neighbor sites, while the CO adsorption energy is actually increased at third-nearest-neighbor sites.⁴² Our results show, however, that oxygen atoms can adsorb on both first- and second-nearest-neighbor sites. The S–O repulsion enforces the order of site occupation but does not block sites. The ability of oxygen to occupy sites that are blocked for CO adsorption may be due to the higher adsorption energy of oxygen; the desorption temperature of CO on Cu(100) is ~ 180 K (Ref. 23) whereas oxygen does not thermally desorb from Cu at any temperature due to its strong chemical bond, greater than 4 eV.⁴⁴

The suppression of oxygen's resistivity contribution at sites near sulfur atoms can be interpreted within Persson's model,^{6,16–20} the fundamental idea of which is that the adsorbates act as diffuse scattering centers for the metal's conduction electrons. For a single adsorbate species, Eq. (1) describes the resistivity change, with Σ interpreted as the scattering cross section per molecule. Allowing for the possibility that Σ varies with coverage, we can define an effective cross section,

$$\Sigma_{\text{eff,O}} = \frac{16}{3} \frac{t}{\ell_B \rho_B} \frac{d\rho}{dn_a} \quad (3)$$

At high oxygen coverage, $\Sigma_{\text{eff,O}}$ is indistinguishable from zero. That does not necessarily mean, however, that the scattering cross section of each additional oxygen atom is actually zero. It is possible that the sulfur-oxygen interaction also reduces the scattering cross section of the nearby sulfur, so that $\Sigma_{\text{eff,O}}$ is a sum of two terms,

$$\Sigma_{\text{eff,O}} = \Sigma_O + \delta\Sigma_S, \quad (4)$$

where Σ_O represents the scattering cross section of the added oxygen atom, while $\delta\Sigma_S$ represents the change in scattering cross section of the adjacent sulfur atom. If $\delta\Sigma_S$ is negative, $\Sigma_{\text{eff,O}}$ could be zero even if Σ_O is not. A similar possibility was proposed to account for the near-zero effective scattering cross section of CO on defect sites.²³

In Persson's analysis, the scattering cross section Σ arises from an adsorbate-derived orbital that overlaps the metal's Fermi level, with width in energy Γ and density of states near the Fermi level, $\rho_a(E_F)$,^{17,21,25}

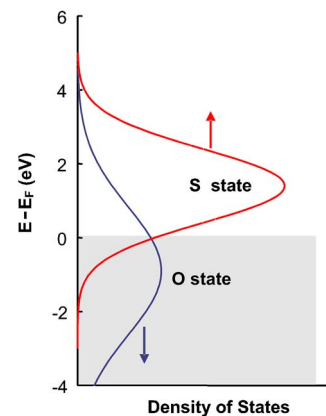


FIG. 5. (Color online) Schematic depiction of the proposed interaction between partially occupied sulfur and oxygen orbitals that could result in the observed resistivity suppression.

$$\Sigma = \frac{16k_F}{3n_B} \langle \sin^2 \theta \rangle_a \Gamma \rho_a(E_F). \quad (5)$$

Here k_F is the Fermi wave vector, n_B is the bulk electron density, and $\langle \sin^2 \theta \rangle_a$ is an average over scattering angles. For a given adsorbate and substrate material, changes in scattering cross section per molecule arise from changes in the width Γ or in the density of states $\rho_a(E_F)$ arising from the adsorbate orbital's overlap with the Fermi level.

The electronic structure and bonding of the individual adsorbates S and O on Cu(100) have been intensively studied,^{45–51} but we are not aware of any studies of the coadsorption system. The O 2p or S 3p orbital hybridizes strongly with the narrow Cu *d* band, and splits into bonding and antibonding components just below and above the *d* band, respectively. Both components are below the Fermi level, as indicated by x-ray emission and photoemission experiments.^{46–50} For sulfur the antibonding state is very narrow (FWHM ~ 0.2 eV), centered approximately 1.5 eV below the Fermi level, and makes little contribution to $\rho_a(E_F)$.^{48,49,51} Consequently, the relatively high surface resistivity of sulfur (see Fig. 1) more likely arises from a broad unoccupied state centered 1.4 eV above the Fermi level, with its low-energy side overlapping the Fermi level.⁴⁹ For oxygen, however, there is evidence of a second, broad antibonding state centered very near the Fermi level.⁵⁰ Oxygen's resistivity contribution probably arises from this partially occupied orbital.

Since the oxygen and sulfur orbitals overlap in energy, quantum mechanical coupling could produce a repulsion in energy between the states, as shown schematically in Fig. 5, shifting both orbitals and modifying the resistivity contribution of each species. Such an effect has been observed for coadsorption of CO and C₂H₄ on Cu(100).²⁵ Since the sulfur orbital lies higher in energy, we would expect the oxygen-derived state to shift to lower energy, reducing its overlap with the Fermi level and lowering its scattering cross section.

Because the oxygen state is broad and centered near E_F ,⁵⁰ however, it seems unlikely that it would shift so much as to reduce the scattering cross section to zero. It is more likely that the observed zero effective cross section $\Sigma_{\text{eff,O}}$ is

due only in part to a reduction in Σ_O . The same interaction that shifts the oxygen orbital to lower energy could also push the sulfur orbital to higher energy, away from the Fermi level. This shift would reduce the cross section of the already adsorbed sulfur ($\delta\Sigma_S < 0$), offsetting the resistivity increase due to the added oxygen atom so that the net change in the sample's resistance is zero. The apparently exact cancellation of the two effects is presumably fortuitous.

Scanning tunneling microscopy studies of both S and O on Cu have shown a strong local perturbation of the local density of states with a full width at half maximum of ~ 1 nm, and a Friedel oscillation at larger distances.^{52,53} For S and O on nearest-neighbor sites, each atom is in a region where the local density of states is strongly perturbed by the other atom, and it is reasonable to expect a relatively strong effect on the states near the Fermi level.

These explanations provide a plausible qualitative account of the observations, but in the absence of experimental or theoretical information on the electronic structure of coadsorbed O and S, they must be considered speculative.

CONCLUSIONS

Measurement of surface resistivity is a useful tool to study the through-metal interactions between two adsorbed atoms. Previous work showed that oxygen and sulfur individually exhibit strikingly different coverage dependences of the surface resistivity—linear for oxygen and saturating at high coverage for sulfur.²⁴ Our experiments show that for oxygen on sulfur-predosed Cu(100), the linear increase of resistivity change with oxygen coverage is strongly suppressed at high coverage, resulting in effectively *zero* resistance change as oxygen adsorbs. The surprising results are attributed to two types of interactions between S and O: S–O repulsion and short-range suppression of surface resistivity.

The experimental data and Monte Carlo simulation jointly reveal several features: the repulsive interaction causes oxygen to adsorb first on sites beyond sulfur's second-nearest-neighbor sites, then on second-nearest-neighbor sites, and finally on sites immediately adjacent to the sulfur atoms. There is strong suppression with almost zero resistivity change when oxygen is on first-nearest-neighbor sites and slight (10%–30%) suppression for second-nearest-neighbor sites, while no resistivity suppression appears for oxygen two or more lattice spacings from sulfur. Thus, the effective range of the suppression is ~ 1.4 lattice spacings (~ 0.36 nm), a factor of 2 smaller than the estimated range of resistivity suppression between sulfur atoms (~ 0.6 – 0.7 nm).²⁴ Monte Carlo simulation also presents a rough lower limit on the energy difference between oxygen adsorption on sulfur's first- and second-nearest-neighbor sites to be greater than about 0.09 eV.

We attribute the suppression of oxygen's surface resistivity contribution to a combination of a reduced electron-scattering cross section of the oxygen itself, and a reduction in the surface resistivity due to the already adsorbed sulfur. Both effects can be qualitatively explained in terms of a coupling between adsorbate-derived orbitals near the Fermi

level. Measurements or calculations of the electronic structure would be very helpful in clarifying the dynamics of this intriguing coadsorption system.

ACKNOWLEDGMENTS

The authors gratefully acknowledge support from Tufts University through a Burlingame graduate fellowship from the Department of Physics and Astronomy (C.L.) and a Faculty Research Award (R.G.T.).

- ¹J. Dvorak, E. Borguet, and H.-L. Dai, *Surf. Sci.* **369**, L122 (1996).
- ²J. Dvorak and H.-L. Dai, *J. Chem. Phys.* **112**, 923 (2000).
- ³C.-L. Hsu, E. F. McCullen, and R. G. Tobin, *Surf. Sci.* **542**, 120 (2003).
- ⁴M. F. G. Hedouin and P. J. Rous, *Phys. Rev. B* **62**, 8473 (2000).
- ⁵A. Dayo, W. Alnasrallah, and J. Krim, *Phys. Rev. Lett.* **80**, 1690 (1998).
- ⁶B. N. J. Persson, *J. Chem. Phys.* **98**, 1659 (1993).
- ⁷J. B. Sokoloff, *Phys. Rev. B* **52**, 5318 (1995).
- ⁸A. I. Volokitin and B. N. J. Persson, *Phys. Rev. Lett.* **94**, 086104 (2005).
- ⁹C. Z. Li, H. Sha, and N. J. Tao, *Phys. Rev. B* **58**, 6775 (1998).
- ¹⁰Z. Liu and P. C. Searson, *J. Phys. Chem. B* **110**, 4318 (2006).
- ¹¹X. Qi and F. E. Osterloh, *J. Am. Chem. Soc.* **127**, 7666 (2005).
- ¹²G. U. Sumanasekera, C. K. W. Adu, S. Fang, and P. C. Eklund, *Phys. Rev. Lett.* **85**, 1096 (2000).
- ¹³V. M. Bermudez, *J. Phys. Chem. B* **109**, 9970 (2005).
- ¹⁴K. Fuchs, *Proc. Cambridge Philos. Soc.* **34**, 100 (1938).
- ¹⁵E. H. Sondheimer, *Adv. Phys.* **1**, 1 (1952).
- ¹⁶B. N. J. Persson, *Surf. Sci.* **269/270**, 103 (1992).
- ¹⁷B. N. J. Persson, *Phys. Rev. B* **44**, 3277 (1991).
- ¹⁸B. N. J. Persson, *Chem. Phys. Lett.* **197**, 7 (1992).
- ¹⁹B. N. J. Persson and A. I. Volokitin, *Surf. Sci.* **310**, 314 (1994).
- ²⁰A. I. Volokitin and B. N. J. Persson, *Phys. Rev. B* **52**, 2899 (1995).
- ²¹R. G. Tobin, *Surf. Sci.* **502–503**, 374 (2002).
- ²²C. J. Hirschmugl, Y. J. Chabal, F. M. Hoffman, and G. P. Williams, *J. Vac. Sci. Technol. A* **12**, 2229 (1994).
- ²³C. Liu and R. G. Tobin, *J. Chem. Phys.* **126**, 124705 (2007).
- ²⁴R. G. Tobin, *Surf. Sci.* **524**, 183 (2003).
- ²⁵M. Hein, P. Dumas, A. Otto, and G. P. Williams, *Surf. Sci.* **465**, 249 (2000).
- ²⁶E. T. Krastev, L. D. Voice, and R. G. Tobin, *J. Appl. Phys.* **79**, 6865 (1996).
- ²⁷E. T. Krastev, D. E. Kuhl, and R. G. Tobin, *Surf. Sci.* **387**, L1051 (1997).
- ²⁸Y. J. Chabal, G. S. Higashi, K. Raghavachari, and V. A. Burrows, *J. Vac. Sci. Technol. A* **7**, 2104 (1989).
- ²⁹G. S. Higashi, R. S. Becker, Y. J. Chabal, and A. J. Becker, *Appl. Phys. Lett.* **58**, 1656 (1991).
- ³⁰P. Dumas, Y. J. Chabal, and G. S. Higashi, *Appl. Phys. Lett.* **65**, 1124 (1990).
- ³¹U. Neuwald, H. E. Hessel, A. Feltz, U. Memmert, and R. J. Behm, *Surf. Sci. Lett.* **296**, L8 (1993).
- ³²M. Nakamura, M.-B. Song, and M. Ito, *Electrochim. Acta* **41**, 681 (1996).
- ³³V. L. Thanh, D. Bouchier, and G. Hincelin, *J. Appl. Phys.* **87**, 3700 (2000).
- ³⁴C.-A. Chang, *J. Appl. Phys.* **67**, 566 (1990).
- ³⁵R. Naik, M. Ahmad, G. L. Dunifer, C. Kota, A. Poli, Ke Fang, U. Rao, and J. S. Payson, *J. Magn. Magn. Mater.* **121**, 60 (1993).
- ³⁶D. E. Kuhl and R. G. Tobin, *Rev. Sci. Instrum.* **66**, 3016 (1995).
- ³⁷K. T. Leung, X. S. Zhang, and D. A. Shirley, *J. Phys. Chem.* **93**, 6164 (1989).
- ³⁸M. L. Colaianni and I. Chorkendorff, *Phys. Rev. B* **50**, 8798 (1994).
- ³⁹K. C. Lin, R. G. Tobin, and P. Dumas, *Phys. Rev. B* **49**, 17273 (1994).
- ⁴⁰M. Wuttig, R. Franchy, and H. Ibach, *Surf. Sci.* **213**, 103 (1989).
- ⁴¹Q. T. Jiang, P. Fenter, and T. Gustafsson, *Phys. Rev. B* **42**, 9291 (1990).
- ⁴²X. F. Hu and C. J. Hirschmugl, *Phys. Rev. B* **72**, 205439 (2005).
- ⁴³S. Stolbov, A. Kara, and T. S. Rahman, *Phys. Rev. B* **66**, 245405 (2002).
- ⁴⁴F. Besenbacher and J. K. Nørskov, *Prog. Surf. Sci.* **44**, 5 (1993).
- ⁴⁵H. Adachi, *Jpn. J. Appl. Phys.* **19**, L527 (1980).
- ⁴⁶G. G. Tibbetts, J. M. Burkstrand, and J. C. Tracy, *Phys. Rev. B* **15**, 3652 (1977).
- ⁴⁷D. T. Ling, J. N. Miller, D. L. Weissman, P. Pianetta, P. M. Stefan,

- I. Lindau, and W. E. Spicer, *Surf. Sci.* **95**, 89 (1983).
- ⁴⁸D. T. Ling, J. N. Miller, D. L. Weissman, P. Pianetta, P. M. Stefan, I. Lindau, and W. E. Spicer, *Surf. Sci.* **124**, 175 (1983).
- ⁴⁹G. Leschik, R. Courths, and H. Wern, *Surf. Sci.* **294**, 355 (1993).
- ⁵⁰T. Wiell, J. E. Klepneis, P. Bennich, O. Bjorneholm, N. Wassdahl, and A. Nilsson, *Phys. Rev. B* **58**, 1655 (1998).
- ⁵¹L. Chiodo and P. Monachesi, *Phys. Rev. B* **75**, 075404 (2007).
- ⁵²P. Avouris, I.-W. Lyo, and P. Molinàs-Mata, *Chem. Phys. Lett.* **240**, 423 (1995).
- ⁵³F. Wiame, V. Maurice, and P. Marcus, *Surf. Sci.* **601**, 1193 (2007).